

# Describing Function Analysis of an Anti-Backlash Controller

Jorge E. Tierno, Kee Y. Kim, Seth L. Lacy and Dennis S. Bernstein

Honeywell Technology Center  
3660 Technology Drive  
Minneapolis MN 55418

Department of Aerospace Engineering  
The University of Michigan  
Ann Arbor MI 48109-2140

## 1 Introduction

Despite advances in design and fabrication, backlash remains a fundamental problem in precision mechanical applications. Deadzone and “play” in mechanical couplings cause hysteretic behavior as can structural components with memory. This behavior can degrade the performance of mechanical systems. When the system involves servo control, backlash can cause undesirable limit cycle oscillations. Our goal in this paper is to present a controller to reduce the effects of backlash.

The effects of backlash are well understood thanks to describing function analysis. The texts [1, 2, 4] provide detailed presentations of this approach. Limit cycle oscillations in control systems involving hysteresis have been studied in [6], while adaptive control methods for suppressing the effects of backlash are studied in [7]. A backlash compensator is given in [3].

In the present paper we develop an anti-backlash controller for servo applications. This controller uses constant feedforward and feedback gains which can be chosen to set the level of control authority. We demonstrate this controller by means of two standard problems, namely, a pure backlash plant as well as a mechanical oscillator with position input through a deadzone. Using time domain analysis, we show that for both of these plants the compensator gains can be chosen to reduce the effects of backlash. Next, using describing function analysis for the linearized frequency response, we show that the controller suppresses the effects of the nonlinearity in reducing phase delay and achieving unity gain in the servo response.

While the describing function technique is classical, the analysis of the anti-backlash controller is nonstandard. Specifically, because of the presence of the feedback junction, gain and phase conditions must be satisfied to characterize the servo response. While these conditions are difficult to solve analytically, we use them to show that the use of high controller authority suppresses the effects of the backlash nonlinearity.

0-7803-5519-9/00 \$10.00 © 2000 AACC

## 2 Anti-backlash Controller

Consider the nonlinear system

$$y = \mathcal{N}(u), \quad (2.1)$$

with the controller shown in Figure 1, where  $\alpha, \beta > 0$ . The control input  $u$  is given by

$$u = (\alpha + 1)r - \beta y, \quad (2.2)$$

where  $y$  is the output of the system and  $r$  is the command. The closed-loop system can be redrawn as in Figure 2. Our goal is to show that the anti-backlash controller reduces the effects of backlash.

Next we let  $\mathcal{N}$  denote a backlash nonlinearity described by

$$y = \max(u, y + d) + \min(u, y - d) - y, \quad (2.3)$$

where  $d$  is half of the width of the backlash (Figure 3). Then the closed-loop system consisting of (2.3) and the control law (2.2) is given by

$$y = \max\left(\frac{\alpha + 1}{\beta + 1}r, y + \frac{d}{\beta + 1}\right) + \min\left(\frac{\alpha + 1}{\beta + 1}r, y - \frac{d}{\beta + 1}\right) - y. \quad (2.4)$$

The closed-loop system is equivalent to a backlash nonlinearity with input  $((\alpha + 1)/(\beta + 1))r$  and backlash width  $d/(\beta + 1)$ . It can thus be seen in Figure 3 that as  $\alpha = \beta \rightarrow \infty$ , the width of the backlash block is reduced to zero.

### 2.1 Describing Function Analysis

In this section we use describing function analysis to investigate the performance of the anti-backlash controller. Suppose that the system is driven by a reference signal  $r(t) = A_r e^{j\omega t}$  and the fundamental harmonic output signal is  $y(t) = A_y e^{j(\omega t + \phi_y)}$ . It can be seen from Figure 2 that the fundamental harmonic control input to the backlash  $u(t) = A_u e^{j(\omega t + \phi_u)}$  satisfies

$$A_u e^{j\phi_u} = (\alpha + 1)A_r - \beta A_y e^{j\phi_y}, \quad (2.5)$$

4164

and the output  $y(t)$  satisfies

$$A_y e^{j\phi_y} = A_u |N(A_u)| e^{j\phi_u} e^{j\angle N(A_u)}, \quad (2.6)$$

where the gain  $|N(A_u)|$  and the phase  $\angle N(A_u)$  of the backlash describing function are given by

$$|N(A_u)| = \begin{cases} 0 & \text{if } A_u < d, \\ \frac{1}{\pi} \sqrt{a^2 + b^2} & \text{if } A_u \geq d, \end{cases} \quad (2.7)$$

$$\angle N(A_u) = \tan^{-1}(a/b) \quad \text{if } A_u \geq d, \quad (2.8)$$

where

$$a = 4\gamma^{-1}(1 - \gamma^{-1}), \quad (2.9)$$

$$b = -\pi + \cos^{-1}(1 - 2\gamma^{-1}) - (1 - 2\gamma^{-1})\sqrt{1 - (1 - 2\gamma^{-1})^2}, \quad (2.10)$$

where  $\gamma \triangleq A_u/d$ .

Using (2.5) and (2.6) we obtain the gain and phase relationships

$$A_u = \sqrt{(\alpha + 1)^2 A_r^2 + \beta^2 A_y^2 - 2(\alpha + 1)\beta A_r A_y \cos \phi_y}, \quad (2.11)$$

$$A_y = A_u |N(A_u)|, \quad (2.12)$$

$$\cos \phi_u = (\alpha + 1) \frac{A_r}{A_u} - \frac{A_y}{A_u} \cos \phi_y, \quad (2.13)$$

$$\phi_y = \angle N(A_u) + \phi_u, \quad (2.14)$$

and

$$\begin{aligned} \frac{A_y}{A_r} &= \frac{\beta^2 |N(A_u)| e^{j\angle N(A_u)}}{(\alpha + 1) e^{j\phi_y} (1 + \beta |N(A_u)| e^{j\angle N(A_u)})} \\ &= \frac{\beta^2 N(A_u)}{(\alpha + 1) |1 + \beta N(A_u) e^{j\angle N(A_u)}|}. \end{aligned} \quad (2.15)$$

**Proposition 2.1** *Let  $A_r > 0$  and  $\alpha = \beta - 1$ . Then the describing function amplitudes of the closed-loop system satisfy*

$$\lim_{\beta \rightarrow \infty} \frac{A_r}{A_y} = 1. \quad (2.16)$$

**Proof:** Suppose  $N(A_u) = 0$ . From (2.12) it follows that  $A_y = 0$ , and thus (2.5) implies  $A_u = \beta A_r$ . If  $\beta > d/A_r$ , we see from (2.5) and (2.7) that  $A_u > d$  and thus  $N(A_u) > 0$ , which is a contradiction. This implies that  $N(A_u) > 0$  for sufficiently large  $\beta$ .

Now suppose  $N(A_u) \rightarrow 0$ . Using (2.7) we obtain  $A_u \rightarrow d$  and from (2.12) we obtain  $A_y \rightarrow 0$ . From (2.5) it follows that

$$A_u = \beta |A_r - A_y e^{j\phi_y}| \geq \beta (A_r - A_y). \quad (2.17)$$

Since  $A_y \rightarrow 0$  the right-hand side approaches  $\infty$  while the left-hand side approaches  $d$ , which is also a contradiction. Thus we conclude that there exists  $\epsilon > 0$  such that  $N(A_u) > \epsilon$ . Therefore,

$$\lim_{\beta \rightarrow \infty} \frac{A_y}{A_r} = \frac{\beta N(A_u)}{|1 + \beta N(A_u) e^{j\angle N(A_u)}|} = 1. \quad \blacksquare$$

For large  $\beta$ , we can use (2.12) to determine the amplitude of the input signal  $u$  for each value of  $A_r$ . For large values of  $A_r$ , it can be seen that  $A_u \approx A_r$ .

## 2.2 Numerical Examples

To demonstrate the closed-loop system for the backlash nonlinearity with the anti-backlash controller shown in Figure 2, we simulate the closed-loop system with increasing values of  $\alpha$  and  $\beta$ . It can be seen from Figure 4 that increasing  $\alpha$  and  $\beta$  reduces the tracking error.

## 3 Damped Rigid Body with Deadzone

Next we consider the damped rigid body with deadzone shown in Figure 5. The equation of motion for the system is given by

$$m\ddot{q}(t) + c\dot{q}(t) - kf_d(u - q(t)) = 0, \quad (3.1)$$

where  $c$  is the damping coefficient,  $k$  is the spring constant and  $d$  is the halfwidth of the deadzone. The deadzone function  $f_d(z)$  is defined by

$$f_d(z) = \begin{cases} z + d & \text{if } z < -d, \\ 0 & \text{if } -d \leq z \leq d, \\ z - d & \text{if } z > d. \end{cases} \quad (3.2)$$

To clarify the relationship between this system and the backlash nonlinearity we let  $u(t) = \sin(\omega t)$  for a decreasing sequence of values of  $\omega$ . Figure 6 demonstrates that under quasi static operation the dynamics of the damped rigid body with deadzone coincides with the dynamics of the backlash nonlinearity [5].

Next we consider the closed-loop system (2.1) and (2.2) with the nonlinear system  $\mathcal{N}(u)$  given by (3.1). The closed-loop system (Figure 7) is given by

$$m\ddot{q}(t) + c\dot{q}(t) - kf_d((\alpha + 1)r - (\beta + 1)q(t)) = 0. \quad (3.3)$$

Letting  $\alpha = \beta$ , (3.3) can be rewritten as

$$m\ddot{q}(t) + c\dot{q}(t) - (\beta + 1)kf_{d/(\beta+1)}(r - q(t)) = 0. \quad (3.4)$$

The closed-loop system is equivalent to the original system with increased spring constant  $(\beta + 1)k$  and decreased deadzone width  $2d/(\beta + 1)$ . It can thus be seen that as  $\beta \rightarrow \infty$ , the width of the deadzone is reduced to zero.

### 3.1 Describing Function Analysis of the Open-loop System

In this section we use describing function analysis to investigate the behavior of the open-loop system

(3.1). Suppose that the system is driven by the signal  $u(t) = A_u e^{j\omega t}$  and the fundamental harmonic output signal is  $y(t) = A_y e^{j(\omega t + \phi_y)}$ . It can be seen from Figure 8 that the fundamental harmonic control input to the deadzone  $e(t) = A_e e^{j(\omega t + \phi_e)}$  satisfies

$$A_e e^{j\phi_e} = A_u - A_y e^{j\phi_y}. \quad (3.5)$$

The output  $y(t)$  satisfies

$$A_y e^{j\phi_y} = A_e N_0(A_e) |G(j\omega)| e^{j\phi_e} e^{j\angle G(j\omega)}, \quad (3.6)$$

where

$$G(j\omega) = \frac{k}{m(j\omega)^2 + c(j\omega)}, \quad (3.7)$$

and the gain  $N_0(A_e)$  of the deadzone describing function is given by

$$N_0(A_e) = \begin{cases} 0 & \text{if } A_e < d, \\ \frac{2}{\pi} (\cos^{-1} \delta^{-1} - \delta^{-1} \sqrt{1 - \delta^{-2}}) & \text{if } A_e \geq d, \end{cases} \quad (3.8)$$

where  $\delta \triangleq A_e/d$ .

Using (3.5) and (3.6) we obtain the gain and phase relationships

$$A_e = \sqrt{A_u^2 + A_y^2 - 2A_u A_y \cos(\phi_u - \phi_y)} \quad (3.9)$$

$$A_y = A_e N_0(A_e) |G(j\omega)|, \quad (3.10)$$

$$\cos \phi_e = \frac{A_u}{A_e} - \frac{A_y}{A_e} \cos \phi_y, \quad (3.11)$$

$$\phi_y = \angle G(j\omega) + \phi_e, \quad (3.12)$$

and

$$\begin{aligned} \frac{A_e}{A_u} &= \frac{1}{e^{j\phi_y} (1 + N_0(A_e) |G(j\omega)| e^{j\angle G(j\omega)})}, \\ &= \frac{1}{|1 + N_0(A_e) |G(j\omega)| e^{j\angle G(j\omega)}|}. \end{aligned} \quad (3.13)$$

Therefore

$$\frac{A_y e^{j\phi_y}}{A_u} = \frac{N_0(A_e) |G(j\omega)| e^{j\angle G(j\omega)}}{(1 + N_0(A_e) |G(j\omega)| e^{j\angle G(j\omega)})}, \quad (3.14)$$

and thus

$$\frac{A_y}{A_u} = \frac{N_0(A_e) |G(j\omega)|}{|1 + N_0(A_e) |G(j\omega)| e^{j\angle G(j\omega)}|}. \quad (3.15)$$

Let  $A_u$  be given. Then, for each choice of  $\omega$ , we compute  $A_e$  and  $N_0(A_e)$  by using (3.8) and (3.13). Now the gain and phase of the left hand side of (3.14) can be determined as shown in Figure 9. Note that at low frequencies the phase plot of (3.14) resembles that of a backlash describing function.

## 3.2 Describing Function Analysis of the Closed-loop System

In this section we use describing function analysis to investigate the effects of the anti-backlash controller. Suppose that the system is driven by a reference signal  $r(t) = A_r e^{j\omega t}$  and the fundamental harmonic output signal is  $y(t) = A_y e^{j(\omega t + \phi_y)}$ . It can be seen from Figure 7 that the fundamental harmonic control input to the damped rigid body with deadzone  $u(t) = A_u e^{j(\omega t + \phi_u)}$  satisfies

$$A_u e^{j\phi_u} = (\alpha + 1)A_r - \beta A_y e^{j\phi_y}, \quad (3.16)$$

and the input to the deadzone  $e(t) = A_e e^{j(\omega t + \phi_e)}$  satisfies

$$A_e e^{j\phi_e} = (\alpha + 1)A_r - (\beta + 1)A_y e^{j\phi_y}, \quad (3.17)$$

and the output  $y(t)$  satisfies

$$A_y e^{j\phi_y} = A_e N_0(A_e) |G(j\omega)| e^{j\phi_e} e^{j\angle G(j\omega)}, \quad (3.18)$$

where the gain  $N_0(A_e)$  of the deadzone describing function is given by (3.8).

Using (3.16)-(3.18) we obtain the gain and phase relationships

$$A_u = \sqrt{(\alpha + 1)^2 A_r^2 + A_y^2 - 2(\alpha + 1)\beta A_r A_y \cos \phi_y}, \quad (3.19)$$

$$A_e = \sqrt{A_u^2 + A_y^2 - 2A_u A_y \cos(\phi_u - \phi_y)}, \quad (3.20)$$

$$A_y = A_e N_0(A_e) |G(j\omega)|, \quad (3.21)$$

$$\cos \phi_u = (\alpha + 1) \frac{A_r}{A_u} - \beta \frac{A_y}{A_u} \cos \phi_y, \quad (3.22)$$

$$\cos \phi_e = \frac{A_u}{A_e} \cos \phi_u - \frac{A_y}{A_e} \cos \phi_y, \quad (3.23)$$

$$\phi_y = \angle G(j\omega) + \phi_e, \quad (3.24)$$

and

$$\begin{aligned} \frac{A_y}{A_r} &= \frac{(\alpha + 1)N_0(A_e) |G(j\omega)| e^{j\angle G(j\omega)}}{e^{j\phi_y} (1 + (\beta + 1)N_0(A_e) |G(j\omega)| e^{j\angle G(j\omega)})} \\ &= \frac{(\alpha + 1)N_0(A_e) |G(j\omega)|}{|1 + (\beta + 1)N_0(A_e) |G(j\omega)| e^{j\angle G(j\omega)}|}. \end{aligned} \quad (3.25)$$

The proof of the following result is analogous to the proof of Proposition 2.1.

**Proposition 3.1** *Let  $A_r > 0$  and  $\alpha = \beta - 1$ . Then the describing function amplitudes of the closed-loop system satisfy*

$$\lim_{\beta \rightarrow \infty} \frac{A_r}{A_y} = 1. \quad (3.26)$$

### 3.3 Numerical Examples

To demonstrate the closed-loop system for the damped rigid body with deadzone with the anti-backlash controller shown in Figure 2, we simulate the closed-loop system with increasing values of  $\alpha$  and  $\beta$ . It can be seen from Figure 10 that increasing  $\alpha$  and  $\beta$  reduces the tracking error.

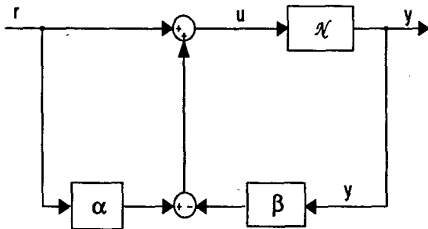


Figure 1: Anti-backlash Controller

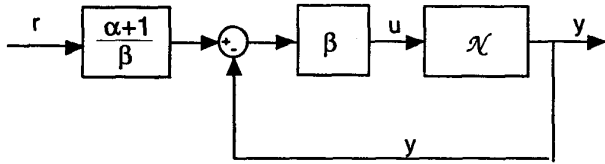


Figure 2: Equivalent Form of the Anti-backlash Controller

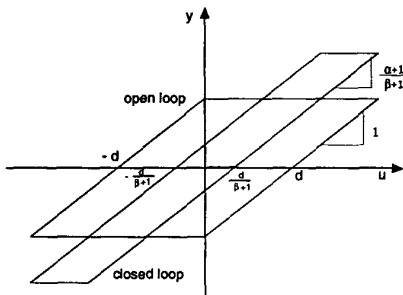


Figure 3: Hysteresis of Backlash Nonlinearity with and without Anti-backlash Controller

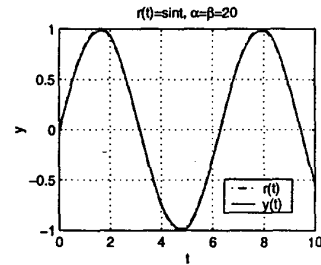
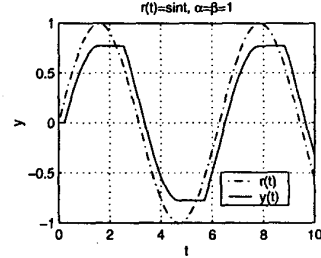


Figure 4: Response of the Closed-Loop System with Backlash Nonlinearity

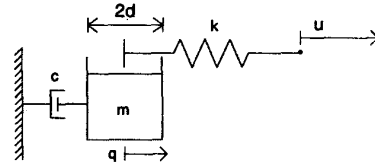


Figure 5: Damped Rigid Body with Deadzone

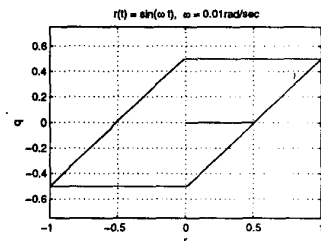
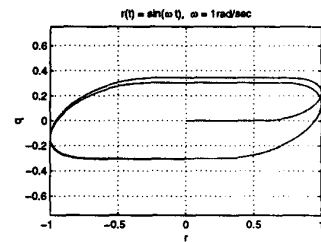


Figure 6: Response of the Damped Rigid Body with Deadzone for a Sequence of Successively Slowing Sinusoidal Input

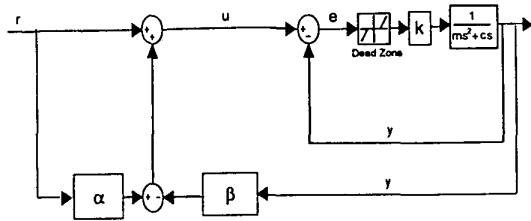


Figure 7: Block Diagram of Closed-Loop System for Damped Rigid Body with Deadzone

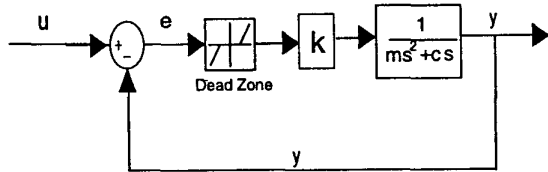


Figure 8: Block Diagram of Damped Rigid Body with Deadzone

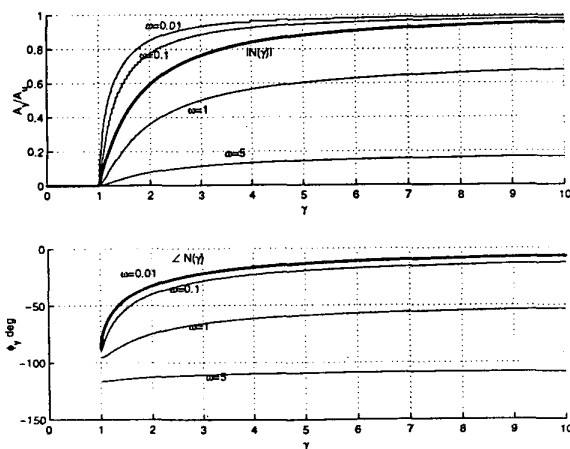


Figure 9: Describing Function of Damped Rigid Body with Deadzone

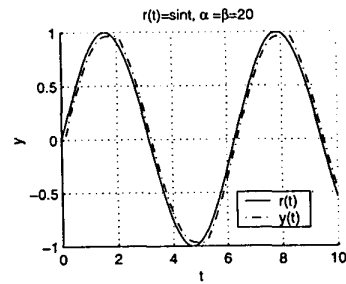
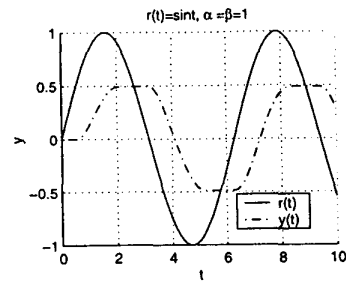


Figure 10: Response of Closed-loop System with Damped Rigid Body with Deadzone

## References

- [1] D. Atherton. *Nonlinear Control Engineering*. Van Nostrand Reinhold, 1982.
- [2] A. Gelb and W. E. V. Velde. *Multiple-Input Describing Functions and Nonlinear System Design*. McGraw-Hill, 1968.
- [3] C. He and Y. Z. L. Xu. Compensation methods for backlash nonlinear characteristics of servo systems. In *Proceedings of 14th IFAC*, 1999.
- [4] W. R. Kolk and R. A. Lerman. *Nonlinear System Dynamics*. Van Nostrand Reinhold, 1992.
- [5] S. L. Lacy, D. S. Bernstein, and S. P. Bhat. Hysteretic systems and step-convergent semistability. Submitted to ACC2000.
- [6] R. K. Miller, A. N. Michel, and G. S. Krenz. On limit cycles of feedback systems which contain a hysteresis nonlinearity. *SIAM Journal on Control and Optimization*, 24(2):276-305, March 1986.
- [7] G. Tao and P. V. Kokotovic. *Adaptive Control of Systems with Actuator and Sensor Nonlinearities*. Wiley, 1996.